Available online at www.sciencedirect.com
ScienceDirect
Journal of Power Sources 174 (2007) 900–904
JOURNAL OF POWER SOURCES
www.elsevier.com/locate/jpowsour

Short communication

Silicon/graphite nanocomposite electrodes prepared by low pressure chemical vapor deposition

Mélanie Alias [a,b], Olivier Crosnier [a], Izabela Sandu [a,c,d], Gwenole Jestin [a], Alexandre Papadimopoulos [a], Frédéric Le Cras [b], Donald M. Schleich [a], Thierry Brousse [a,*]

[a] *Laboratoire de Génie des Matériaux, Ecole Polytechnique de l'Université de Nantes, Nantes Atlantique Universités, La Chantrerie, rue Christian Pauc, BP 50609, 44306 Nantes Cedex 3, France*
[b] *CEA Grenoble, LITEN, 17 rue des Martyrs, 38054 Grenoble Cedex 9, France*
[c] *Institut des Matériaux Jean Rouxel (IMN), UMR 6502, 2 rue de la Houssinière, BP 32229, 44322 Nantes Cedex 3, France*
[d] *INRS Énergie, Matériaux et Télécommunications, 1650 boulevard Lionel Boulet, Varennes J3X 1S2, Québec, Canada*

Available online 27 June 2007

Abstract

Silicon-coated carbon has been prepared by low pressure chemical vapor deposition (LPCVD) using silane as the precursor gas. A porous homogeneous layer made of spherical shaped particles was deposited. The average silicon particle diameter varied from 5 to 30 nm depending upon deposition conditions. Theoretical calculations have been performed to determine the capacity of graphite/silicon electrodes according to the shape of graphite flakes and to the thickness of the silicon layer. This calculation shows that even a minor amount of silicon is efficient in enhancing the capacity of the composite electrode. The electrochemical performance of carbon/silicon composite electrodes has been investigated by charge/discharge galvanostatic tests and cyclic voltammetry experiments. A small amount of silicon (3.6 wt%) leads to an increase of the capacity of the graphite electrode (+27%) without significant impact on the cyclability, thus combining the effect of both materials. Increasing the silicon content (10.7 wt%) leads to an initial capacity of 780 mAh g^{-1} but it strongly affects the cycling ability of the composite negative electrode.

Keywords: Silicon; Negative electrode; Lithium ion battery; Chemical vapor deposition; Graphite; Coating

1. Introduction

Graphite is a common material used as negative electrode in lithium-ion batteries with good cyclability. However, theoretical capacity is limited to 372 mAh g^{-1} or 930 Ah L^{-1}. Moreover, during the first cycle, the formation of a solid electrolyte interface (SEI) leads to an irreversible capacity [1].

To increase the specific energy of lithium-ion batteries, alternative active materials for negative electrodes have been tested. Silicon is one of the most promising materials which combines low-molecular weight and lithium rich binary alloys [2]. Obrovac and Christensen [3] has determined that the composition of the lithium richest alloy that can form at room temperature is $Li_{15}Si_4$, with a corresponding theoretical capacity of 3578 mAh g^{-1}. Unfortunately, the huge volume change during the lithium alloying reaction leads to cracking and crumbling of the silicon particles [4]. Consequently, capacity abruptly fades after only a few charge/discharge cycles. To circumvent this problem, several research efforts have been carried out to disperse fine silicon particles within the graphite matrix by different techniques including mechanical milling [5], formation of silicon-metal composites [6], pyrolysis [7], thermal vapor decomposition [8,9], chemical reaction of gel [10], and chemical vapor deposition (CVD) [11–15]. A review of all these methods has been recently published [16]. The key point is to combine the extra-capacity due to silicon with the good cycling ability of graphite. Concomitantly to these efforts, many studies have been undertaken to determine the lithium–silicon reaction schemes in order to limit or cancel the drawbacks of silicon based anodes and to enhance their cycling ability [17].

Usually, when large amounts of silicon are used, an irreversible capacity is observed during the initial cycle and rapid fade in specific capacity occurs. Research strategies are now focused toward the intimate formation of a carbon/silicon

* Corresponding author.
E-mail address: thierry.brousse@univ-nantes.fr (T. Brousse).

0378-7753/$ – see front matter © 2007 Elsevier B.V. All rights reserved.
doi:10.1016/j.jpowsour.2007.06.088

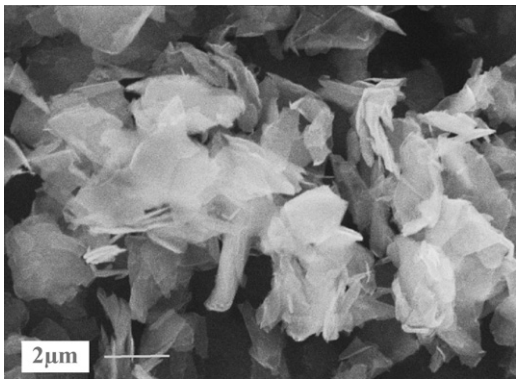

Fig. 1. SEM micrograph of SFG6 graphite.

mixture with limited silicon amount in order to balance the improvement of graphite capacity and maintain the cyclability of the composite electrodes. Some example can be found in the literature with moderate amounts of silicon (0.05–15%) deposited onto graphite flakes [11–15]. Holzapfel and co-workers [12–15] report in several papers the CVD deposition of silicon onto graphite, with a noticeable enhancement of capacity and cycling ability.

In the present study, silicon-coated graphite has been prepared by low pressure chemical vapor deposition. The expected increase of the reversible capacity of graphite is calculated from a theoretical point of view according to the deposited amount of silicon in the composite material. Our expectation is that the combination of a small amount of nanosized silicon particles together with graphite matrix leads to improved capacity as well as good cycling ability.

Prior to the experiments, the capacity of the composite was calculated according to the shape of the graphite particles (Fig. 1) determined from scanning electron microscopy (SEM), and to the thickness of the silicon layer. A single graphite flake is considered as a prismatic grain, with a thickness h greater than the deposited silicon layer, e. To simplify the calculation, silicon is supposed to cover only the two basal planes of the graphite flakes. The total capacity is expressed as

$$Q_t = \frac{m_C \times Q_C + m_{Si} \times Q_{Si}}{m_c + m_{Si}}$$

$$Q_t = \frac{\rho_C \cdot h \cdot 372 + 2\rho_{Si} \cdot e \cdot 3578}{\rho_C \cdot h + 2\rho_{Si} \cdot e}$$

with Q as the specific capacity (Q_c for graphite, 372 mAh g^{-1} and Q_{Si} for silicon, 3578 mAh g^{-1} corresponding to $Li_{15}Si_4$); h the thickness of graphite flakes (0.25 μm); e the thickness of the silicon layer; ρ_c and ρ_{Si} are the densities of graphite (2.26 g cm^{-3}) and silicon (2.33 g cm^{-3}), respectively.

The total capacity versus the thickness of the silicon layer is calculated in Fig. 2. Two regimes can be distinguished. Below 10 nm, the silicon brings a small but noticeable capacity to graphite. Above 10 nm, the capacity increases drastically as thicker films are grown. For example, a 30 nm thin layer of silicon can lead to a theoretical capacity of 1000 mAh g^{-1} which is nearly three times the capacity of pure graphite.

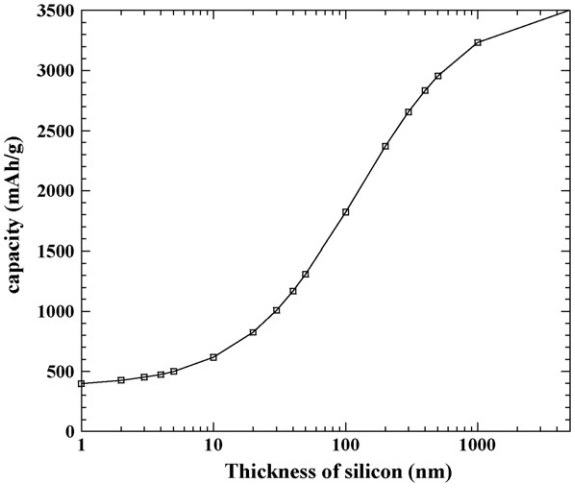

Fig. 2. Theoretical capacity of graphite/silicon composite electrodes as a function of silicon layer thickness.

2. Experimental

Si-coated graphite (SFG6 grade, TIMCAL, Switzerland) was synthesized by low pressure chemical vapor deposition (LPCVD). Prior to the CVD process, graphite powder with an average particle size of 6 μm was spread on a tilted substrate holder in order to obtain a homogeneous thickness (Fig. 3). The substrate holder was put in the middle of the reactor. Silane diluted in 90% argon and Ar/H_2 were mixed in the reactor. Silane was thermally decomposed at 650 °C and silicon nanoparticles covered the surface of the graphite flakes. After 45 min of deposition, the reactor was switched off and cooled down to room temperature. The Si-coated graphite powder was mixed and reintroduced into the reactor. The CVD process was performed several times, removing the sample between each deposition to obtain a homogeneous composite powder.

Two samples were synthesized: SFG4/4 corresponds to 4 depositions of 45 min each. SFG6 6/6 corresponds to 6 depositions of 1 h each. The average size of silicon particles was estimated according to SEM and TEM observations. The composition was determined by thermogravimetric analysis (TGA) performed under an air atmosphere with a heating rate 5 °C min^{-1} up to 850 °C.

The electrochemical behavior of composite electrodes was investigated using a Mac Pile II (Bio-Logic) in an argon-filled

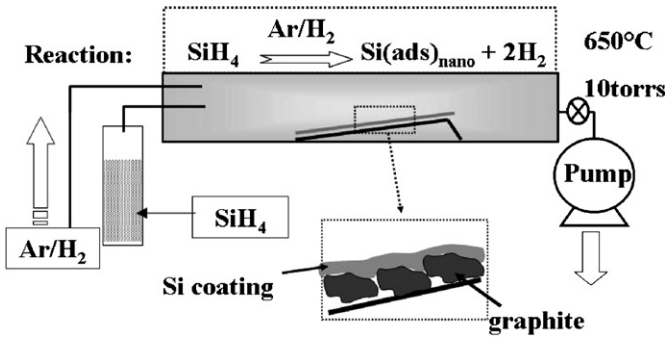

Fig. 3. Schematic view of the CVD equipment.

glove box. Both galvanostatic and potentiostatic tests were performed. The working electrodes were prepared as follows: Si-coated graphite powder (80 wt%), acetylene black (10 wt%) and PVDF (10 wt%) dissolved in NMP were mixed together to obtain a slurry which was spread onto a copper foil. The electrodes were dried at 85 °C for 12 h. A lithium disk was used as both the counter and reference electrode. The electrolyte (1M $LiPF_6$ in EC:DEC) was supported by a glass paper fiber separator.

3. Results and discussion

Fig. 4 shows the SEM micrographs of Si-coated SFG6 with different deposition times. Rather than a homogeneous layer, the deposit is made of tiny spherical silicon particles. As can be seen from the SEM micrographs, longer deposition times result in thicker silicon layers. For SFG6 4/4 silicon nanoparticles, <10 nm in diameter, cover the graphite surface whereas for SFG6 6/6 the average particle size is around 30 nm (estimated from SEM micrographs). These values are confirmed by TEM observations. As an example, the surface of a SFG6 4/4 grain is shown in Fig. 4c. Tiny silicon particles, ≈5 nm diameter, are identified by micro-EDX and electron diffraction. Since a continuous thin film is not prepared, the previous theoretical calculation cannot be used directly with the silicon layer thickness, but was modified to integrate the silicon weight content instead.

TGA analyses show that the samples SFG6 4/4 and SFG6 6/6 contain 3.6 ± 0.4 and 10.7 ± 1.0 wt% silicon, respectively. This confirms that the silicon content in the composite SFG6 6/6 is larger than in SFG6 4/4.

Cyclic voltammograms of the first two cycles of the pristine graphite and of the Si-graphite composites in lithium-ion cells are shown in Fig. 5. In Fig. 5a, reduction and oxidation peaks in the range 0–0.25 V/Li+/Li are consistent with the reversible formation of Li_xC_6 intercalation stages. This behavior is in good agreement with the lithiation process of graphite described by Aurbach et al. [18]. The anodic peak obtained at 0.45 versus Li/Li^+ and the cathodic peak (Fig. 5c) at 0.2 V/0.3 V are assigned to the formation of Li–Si alloys.

Fig. 6 compares the cycling behavior of pure graphite (SFG6) and Si-graphite composite electrodes. Although SFG6 6/6 exhibits significantly larger reversible capacity (800 mAh g^{-1}) than the SFG6 sample (≈300 mAh g^{-1}). This initial capacity value for SFG6 6/6 sample is very close to that expected from our theoretical calculation (782 mAh g^{-1}), which is consistent with the silicon amount determined in this sample. The capacity fades very rapidly especially in the initial cycles (from 780 to 545 mAh g^{-1} after 10 cycles). Assuming the capacity of graphite is 300 mAh g^{-1}, these values translate into ≈50% drop in capacity of silicon after only 10 cycles, which is in the range usually found in the literature data for pure silicon active material [19]. This is probably due to the microstructure of the SFG6 6/6 sample. Indeed, the silicon nanoparticles formed a dense layer on the surface of the graphite flakes, without empty spaces on the surface to allow 3D volume expansion. The result is an electrochemical behavior close to the one experienced by bulk silicon particles.

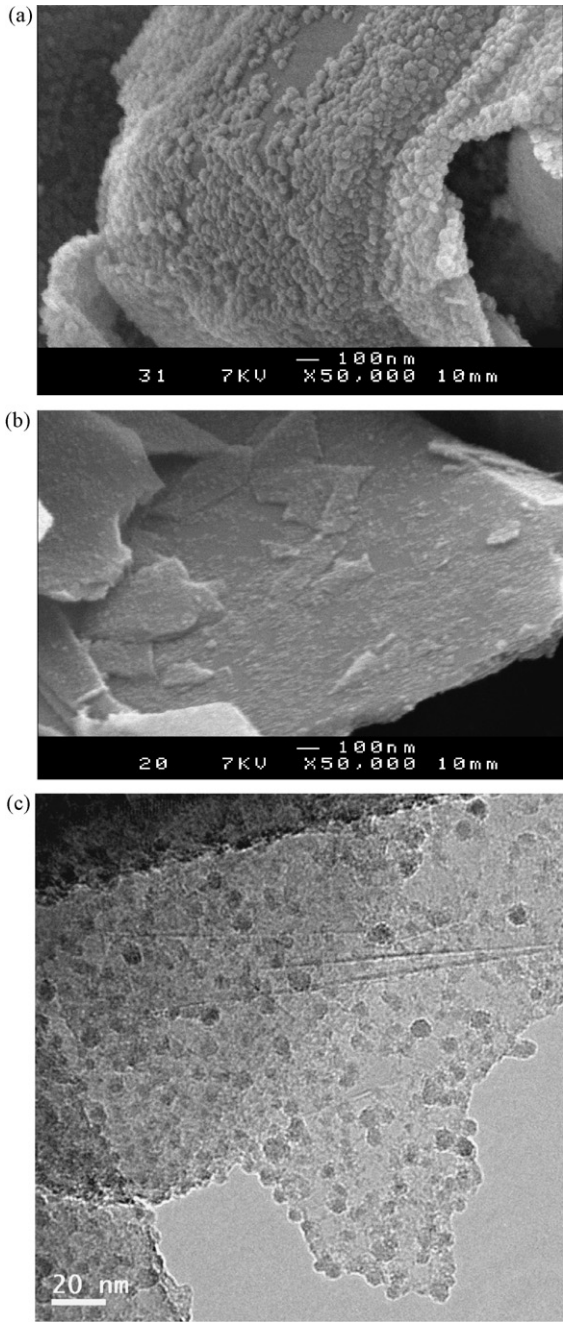

Fig. 4. SEM image of (a) SFG6 6/6 (6 × 1 h), (b) SFG6 4/4 (4 × 3/4 h), and (c) TEM detail of sample SFG6 4/4 (4 × 3/4 h): small spherical silicon particles on a surface of a graphite sheet.

For SFG6 4/4, the reversible capacity decreases from 437 mAh g^{-1} in the first cycle to 377 mAh g^{-1} after the 10th cycle. Compared to graphite, the composite electrode shows a 27% gain in capacity for 3.6 wt% silicon. The initial capacitance value is slightly lower than expected from theoretical calculations (510 mAh g^{-1}). The relative better stability of SFG6 4/4 compared to SFG6 6/6 is probably due to some extend to a more favorable microstructure (Fig. 4b and c) which allows, unlike SFG6 6/6, a 3D expansion of silicon nanoparticles. Additionally the smaller size of silicon particles helps to sustain volume expansion upon cycling. However, the SFG6 4/4 sample still

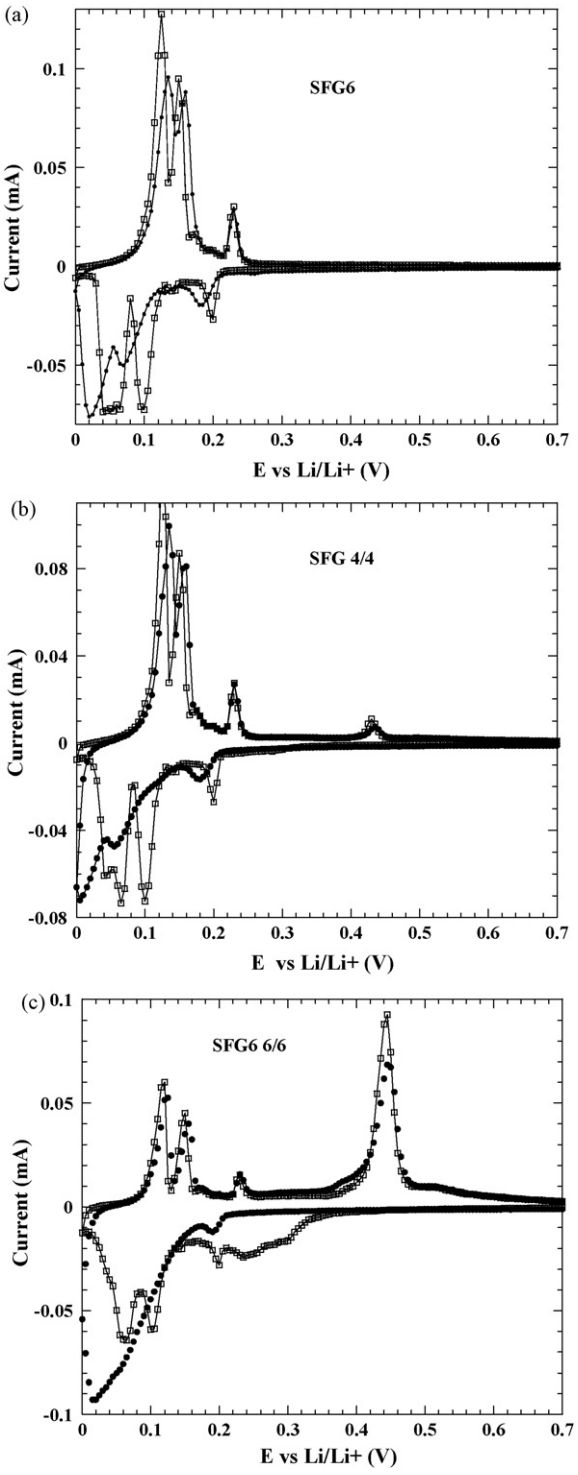

Fig. 5. First cycle (black round) and second cycle (square) cyclic voltammograms of SFG6 (a), composite SFG6 4/4 electrode (b), and SFG6 6/6 electrode (c). Sweep rate is 10 mV h^{-1}.

exhibits a capacity fade upon cycling, and other parameters have to be optimized to improve the composite electrode stability, such as the chemical bond between graphite and silicon particles. It must be noted than unlike other studies which show superior cycling ability with capacity around 500 mAh g^{-1} [12–15], no special cycling conditions such as current monitoring at the end of discharge have been used to limit capacity fade.

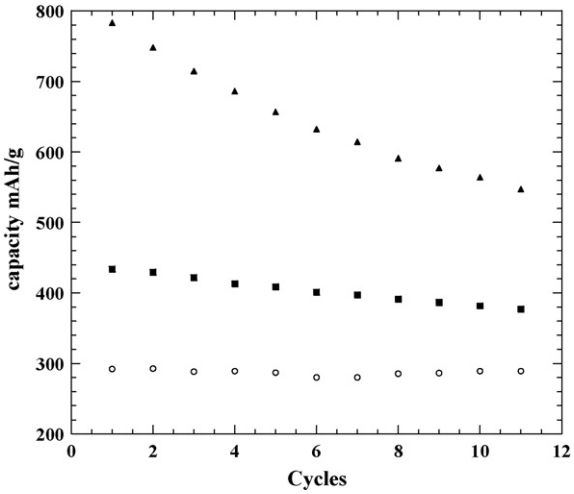

Fig. 6. Charge capacity (C/5 rate) for graphite (open circles), graphite with 3.6 wt% silicon (black squares), and 10.7 wt% silicon (black triangles).

The cycling behavior of the composite electrode depends on silicon content and on the microstructure of the deposit. The composite behaves as a pure silicon film if the Si amount is too important whereas low silicon content allows an increase of capacity with improved cyclability.

4. Conclusion

Our goal was to prepare silicon/graphite composite electrodes in order to combine the high capacity of silicon and the good cyclability of graphite. Depending upon the deposition conditions and silicon amount, a porous homogeneous layer made of 5–30 nm spherical shaped silicon particles was observed. Cyclic voltammetry clearly demonstrates that silicon participates in the lithiation and delithiation reactions of the composite electrodes. A 27% gain in capacity is obtained for only 3.6 wt% of Si, thus indicating that composite silicon/graphite electrodes can combine the advantages of both components, but efforts are still required to improve their cyclability.

References

[1] R. Fong, U. von Sacken, J.R. Dahn, J. Electrochem. Soc. 137 (1990) 2009.
[2] C.J. Wen, R.A. Huggins, J. Solid State Chem. 37 (1981) 271.
[3] M.N. Obrovac, L. Christensen, Electrochem. Solid State Lett. 7 (2004) A93.
[4] J.H. Ryu, J.W. Kim, Y.-E. Sung, S.M. Oh, Electrochem. Solid State Lett. 7 (2004) A306.
[5] C.S. Wang, G.T. Wu, X.B. Zhang, Z.F. Qi, W.Z. Li, J. Electrochem. Soc. 145 (1998) 2751.
[6] L.Y. Beaulieu, K.C. Hewitt, R.L. Turner, A. Bonakdarpour, A.A. Abdo, L. Christensen, K.W. Eberman, L.J. Krause, J.R. Dahn, J. Electrochem. Soc. 150 (2003) A149.
[7] X. Zhang, P.K. Patil, C. Wang, A.J. Appleby, F.E. Little, D.L. Cocke, J. Power Sources 125 (2004) 206.
[8] M. Yoshio, H. Wang, K. Fukuda, T. Umeno, N. Dimov, Z. Ogumi, J. Electrochem. Soc. 149 (2002) 1598.
[9] X.O. Yang, J. McBreen, W.S. Yoon, M. Yoshio, H. Wang, K. Fukuda, T. Umeno, Electrochem. Commun. 4 (2002) 893.

[10] G.X. Wang, J.H. Ahn, J. Yao, S. Bewlay, H.K. Liu, Electrochem. Commun. 6 (2004) 689.
[11] J. Xie, G.S. Cao, X.B. Zhao, Mater. Chem. Phys. 88 (2004) 295.
[12] M. Holzapfel, H. Buqa, W. Scheifele, P. Novak, F.-M. Petrat, Chem. Commun. (2005) 1566.
[13] H. Buqa, D. Goers, M. Holzapfel, M.E. Spahr, P. Novak, J. Electrochem. Soc. 152 (2005) A474.
[14] M. Holzapfel, H. Buqa, F. Kruneich, P. Novak, F.-M. Petrat, C. Veit, Electrochem. Solid State Lett. 8 (2005) A516.
[15] M. Holzapfel, H. Buqaa, L.J. Hardwick, M. Hahna, A. Würsig, W. Scheifele, P. Novák, R. Kötz, C. Veit, F.-M. Petrat, Electrochim. Acta 52 (2006) 973.
[16] U. Kasavajjula, C. Wang, A.J. Appleby, J. Power Sources 163 (2006) 1003.
[17] J. Lia, J.R. Dahn, J. Electrochem. Soc. 154 (2007) A156.
[18] D. Aurbach, B. Markovsky, I. Weissmana, E. Levi, Y. Ein-Elib, Electrochim. Acta 45 (1999) 67.
[19] S. Bourderau, T. Brousse, D.M. Schleich, J. Power Sources 81/82 (1999) 233.